Eur. Phys. J. A (2009)
DOI 10.1140/epja/i2009-10835-1

THE EUROPEAN PHYSICAL JOURNAL A

Regular Article – Experimental Physics

Preparing a journey to the east of ^{208}Pb with ISOLTRAP: Isobaric purification at A = 209 and new masses for $^{211-213}$Fr and ^{211}Ra

M. Kowalska[1,a], S. Naimi[2], J. Agramunt[3], A. Algora[3,4], G. Audi[2], D. Beck[5], B. Blank[6], K. Blaum[7], Ch. Böhm[7], M. Breitenfeldt[9], E. Estevez[3], L.M. Fraile[10], S. George[7,8], F. Herfurth[5], A. Herlert[1], A. Kellerbauer[7], D. Lunney[2], E. Minaya-Ramirez[2], D. Neidherr[7], B. Olaizola[10], K. Riisager[11], M. Rosenbusch[9], B. Rubio[3], S. Schwarz[12], L. Schweikhard[9], and U. Warring[7]

[1] CERN, Physics Department, 1211 Geneva 23, Switzerland
[2] CSNSM-IN2P3-CNRS, Université de Paris Sud, Orsay, France
[3] IFIC, CSIC-Universidad de València, 46071, Spain
[4] Institute of Nuclear Research of the Hungarian Academy of Sciences, 4026 Debrecen, Hungary
[5] GSI Helmholtzzentrum für Schwerionenforschung GmbH, Planckstrasse 1, 64291 Darmstadt, Germany
[6] CENBG, Université Bordeaux 1/CNRS/IN2P3, 33175 Gradignan Cedex, France
[7] Max-Planck-Institut für Kernphysik, 69117 Heidelberg, Germany
[8] Johannes Gutenberg-Universität, Institut für Physik, 55099 Mainz, Germany
[9] Ernst-Moritz-Arndt-Universität, Institut für Physik, 17487 Greifswald, Germany
[10] Universidad Complutense, Departamento de Física Atómica, Molecular y Nuclear, 28040 Madrid, Spain
[11] University of Aarhus, Department of Physics and Astronomy, 8000 Aarhus, Denmark
[12] NSCL, Michigan State University, East Lansing, MI, USA

Received: 5 January 2009 / Revised: 12 May 2009

Communicated by C. Signorini

Abstract. With the Penning trap mass spectrometer ISOLTRAP, located at ISOLDE/CERN, preparatory work has been performed towards mass and decay studies on neutron-rich Hg and Tl isotopes beyond $N = 126$. The properties of these isotopes are not well known because of large isobaric contamination coming mainly from surface-ionised Fr. Within the studies, production tests using several target-ion source combinations were performed. It was furthermore demonstrated around mass number $A = 209$ that the resolving power required to purify Fr is achievable with ISOLTRAP. In addition, masses of several isobaric contaminants, $^{211-213}$Fr and ^{211}Ra, were determined with a three-fold improved precision. The results influence masses of more than 20 other nuclides in the ^{208}Pb region.

PACS. 21.10.Dr Binding energies and masses – 27.80.+w $190 \leq A \leq 219$ – 32.10.Bi Atomic masses, mass spectra, abundances, and isotopes

1 Introduction

Isotope Separation On Line (ISOL) facilities can produce superior yields for many nuclides of interest over the nuclear chart. However, ISOL beams are often accompanied by large isobaric contaminations. In regions where sufficient purification cannot be achieved on the target and ion-source side, Penning trap mass spectrometers turn out to be ideal purifiers. Penning traps are present at many on-line facilities [1] and can reach a resolving power $m/\Delta m$ of over 10^5, which allows resolving and purifying most unwanted isobars [2] and in some cases even isomers [3–5]. This feature has been extensively used to perform high-precision mass measurements. Recently it has been also shown that mass purification in a Penning trap can assist decay spectroscopy studies of exotic nuclei [6]. The combination of Penning trap mass spectrometry and decay spectroscopy can enhance the strong discovery potential of the former, as recently shown: for the first time a new isomer [7] and even a new nuclide [8] have been identified with the LEBIT and ISOLTRAP Penning trap setups.

Following these recent achievements, it is envisaged to investigate nuclides south-east from ^{208}Pb —with $Z < 82$ and $N > 126$, especially the neutron-rich Hg and Tl isotopes, using the purification capabilities of the ISOLTRAP setup. The studies of these nuclides

[a] e-mail: kowalska@cern.ch

Published online: 26 July 2009

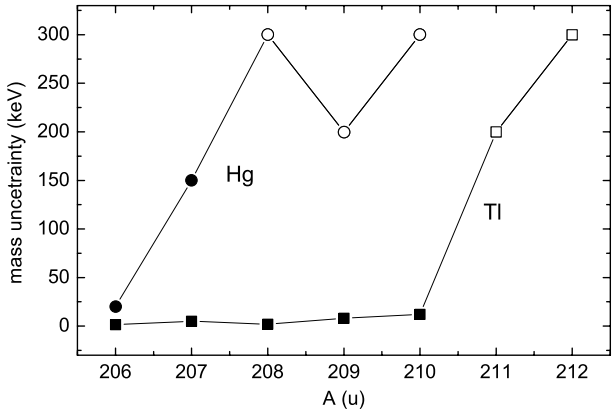

Fig. 1. Experimental uncertainty in the mass of neutron-rich Hg and Tl isotopes [12] before our studies. Until 2008 none of the masses were measured directly (when the mass of ^{208}Hg was measured using the Schottky mass spectrometry at GSI [13]). Data represented by empty circles and squares are derived not from purely experimental data, but at least partly from systematic trends.

are presently hampered by a very strong contamination by surface-ionised Fr and Ra isotopes. Separating these species requires a mass-resolving power of 10^4–10^5 (see table 3), routinely achieved at ISOLTRAP. In addition to conventional mass spectrometry, β- and γ-decay schemes will be investigated, using a tape-transport system presently being commissioned at ISOLTRAP. With this setup, the identification of new isotopes and isomers should also be feasible. Predictions for half-lives of many yet unidentified Hg and Tl isotopes are in the range of seconds [9,10], and the region is rich in long-lived isomers (*e.g.*, $t_{1/2}$ of 3.7 min for ^{206}Tl and 1.3 s for ^{207}Tl), due to the proximity of proton orbits with very different spin values (see sect. 2).

In this paper we discuss preparatory work, comprising production tests for neutron-rich Hg and Tl isotopes, and for the undesired isobars as well as checks of the purification capabilities of ISOLTRAP. In addition, we present improved mass values of several nuclides in the $A = 208$ region which resulted from these tests and show their influence on a dozen more masses. Finally, we give an outlook concerning the mass studies and the trap-assisted decay measurements on the Hg and Tl isotopes.

2 Physics motivation

2.1 Masses

Unlike masses of nuclides west of ^{208}Pb, which were studied extensively with ISOLTRAP [11], the masses of Hg and Tl isotopes beyond $N = 126$ are not very well known [12]. Their uncertainties (excepting $^{206-210}$Tl and ^{208}Hg) are in the range of several hundred keV, as shown in fig. 1. Until recently none of them have been measured directly (in 2008 the mass of ^{208}Hg was measured using the Schottky mass spectrometry at GSI [13]) and the majority is determined based on systematic trends.

The reliability of mass extrapolations into regions of unknown nuclei is of interest for many aspects of nuclear structure and is particularly important for astrophysical applications. In this respect, mass measurements around ^{208}Pb are extremely valuable, since predictions for different terms in the mass formulas, such as the isospin symmetry term, vary significantly for different models. Moreover, this effect increases when going from one shell to another, as shown recently [14].

Due to the proximity of closed shells, the masses in this section of the nuclear chart are also important for the valence proton-neutron interaction (p-n), which depends strongly on the spatial overlap of the proton and neutron orbits. The average interaction strength of the last proton(s) with the last neutron(s), denoted δV_{pn}, can be isolated from double mass differences, as shown below for even-even and even Z - odd N nuclei [15,16], respectively:

$$\delta V_{pn}^{ee}(Z,N) = \frac{1}{4}[(B_{Z,N} - B_{Z,N-2}) - (B_{Z-2,N} - B_{Z-2,N-2})],$$

$$\delta V_{pn}^{eo}(Z,N) = \frac{1}{2}[(B_{Z,N} - B_{Z,N-1}) - (B_{Z-2,N} - B_{Z-2,N-1})]$$

where B is the binding energy.

It has been shown that the p-n interaction reflected in δV_{pn} is crucial for the development of configuration mixing, for changes of the underlying shell structure [17], and for the onset of collectivity and deformation in nuclei [18] (*e.g.*, recently, large δV_{pn} were observed for Ra isotopes around $A = 224$ [8] which are known to exhibit octupole deformation). If the p-n interaction is indeed influenced mainly by the spacial overlap of the proton and neutron orbits, the δV_{pn} values should change abruptly when going from one shell to another. The first experimental value for nuclei with $N > 126$ and $Z < 82$ was added in 2008 based on the mass of ^{208}Hg measured at GSI-Darmstadt [13]. The derived δV_{pn} for Pb is only 165 keV, as expected for a small overlap of p-n orbits. The masses of other neutron-rich Hg and Tl isotopes will provide more experimental δV_{pn} values in this region.

Masses beyond $N = 126$ will also complement the extensive studies on the other side of this magic number which were performed previously at ISOLTRAP [11,19]. Furthermore, with future laser spectroscopy data of neutron-rich Hg and Tl isotopes, the discussion of possible correlations between binding energies and charge radii, as presented by Weber *et al.* [11] for nuclides west of ^{208}Pb, will be for the first time possible south-east of this nuclide.

2.2 Decay data

The present knowledge of the excited states of neutron-rich Tl and Pb isotopes (Hg and Tl daughter nuclides) is summarised in table 1 and table 2. In some cases no decay information is available at all, and even the ground-state half-life is not known.

Table 1. Measured nuclear-structure properties of neutron-rich Tl isotopes [20–22].

A	N	I^π	$t_{1/2}$ g.s./isomer	Level scheme known from α-/β-decay
206	125	0^-	3.7/4.2 min	yes/yes
207	126	$1/2^+$	1.3 s/4.8 min	yes/yes
208	127	5^+	3.1 min	yes/yes
209	128	$(1/2^+)$	2.2 min	yes/no[a]
210	129	(5^+)[b]	1.3 min	no/no
211	130	$(1/2^+)$[b]	>300 ns	no/no
212	131	–	>300 ns	no/no

[a] L. Zhang *et al.* [23] observed 3 new γ lines in the β-decay of ^{209}Hg, which they attributed to ^{209}Tl, but no new level scheme was proposed.
[b] Derived from systematics.

Table 2. Measured nuclear-structure properties of neutron-rich Pb isotopes [22].

A	N	I^π	$t_{1/2}$	Level scheme known from α-/β-decay
209	127	$9/2^+$	3.3 h	yes/yes
210	128	0^+	22.3 years	yes/yes
211	129	9/2+	36.1 min	yes/no
212	130	0^+	10.6 h	yes/no
213	131	$(9/2^+)$	10.2 min	yes/no
214	132	0^+	26.8 min	yes/no
215	133	–	–	no/no

The decay studies will give access to the positions of the single-particle states and their evolution with an increasing number of protons. Tl isotopes have 81 protons, thus their ground state should be formed by one proton hole in one of the close-lying $h_{11/2}s_{1/2}d_{3/2}$ orbits below the $Z = 82$ shell gap. For even mass —and odd neutron— isotopes beyond $A = 206$ this hole is coupled to a neutron in one of the $g_{9/2}d_{3/2}i_{11/2}$ orbits. Lead isotopes with $Z = 82$, on the other hand, are magic and their low-lying nuclear structure —beyond doubly magic ^{208}Pb— should be governed only by valence neutrons above $N = 126$. At higher energies, also excitation of protons across $Z = 82$ may take place.

Studies of level schemes of nuclides with few valence particles or holes provide the best test ground for basic ingredients of shell model calculations, especially concerning the matrix elements of the two-body residual interaction. In the case of neutron-rich Hg and Tl isotopes, which have been particularly successfully described by Kuo and Herling [24], new information can be gained on the interaction of proton holes with neutron particles. Since the data are so scarce, every new decay measurement can be used to refine and improve the existing interactions [25,26]. It also allows to trace the evolution of the single-particle levels when going away from the doubly magic ^{208}Pb, and to clarify to which extent the shell model with magic $Z = 82$ and $N = 126$ is upheld in this region.

3 Experimental procedure

The mass and decay studies of the Hg and Tl isotopes are planned at the double Penning trap mass spectrometer ISOLTRAP [27] (fig. 2) located at the on-line isotope separator facility ISOLDE at CERN. The radionuclides of interest are produced by nuclear reactions induced in a thick target by pulses of up to 3×10^{13} protons at an energy of 1.4 GeV from CERN's Proton Synchrotron Booster accelerator. After diffusion out of the heated target container they are ionised on a hot surface, via electron impact, or by selective resonant laser excitation, extracted and accelerated to energies between 30 and 60 keV, mass separated in one or two dipole magnets, and finally guided to the ISOLTRAP setup (fig. 2).

The experimental procedure at ISOLTRAP is the following: a linear gas-filled radiofrequency quadrupole (RFQ) ion trap [28] captures the continuous ISOLDE beam and prepares it for transfer into the preparation Penning trap. To this end, the ISOLDE ions are electrostatically retarded before they enter the RFQ, where they are cooled by energy loss due to collisions with the He buffer gas. After a certain cooling time (typically 10 ms) the ions are transferred as an ion bunch into the tandem Penning trap system.

In Penning traps the ion selection and mass determination are based on the cyclotron frequency $\nu_c = qB/(2\pi m)$ of the studied ion. Here, q and m are the charge state and the mass of the ion, respectively, and B is the magnetic field.

3.1 Preparation Penning trap

In the preparation Penning trap the ions are stored and the contaminant ions are removed using the mass-selective cooling in the presence of a buffer gas [29] (in our case, He). The procedure is the following: all ions present in the trap are brought to a radius larger than the 4 mm aperture in the upper endcap of the trap. Then, only the ions of interest are centered using a mass-selective quadrupole excitation at their cyclotron frequency ν_c and are ejected through the diaphragm. The resulting resolving power reaches 10^5 (for 1 s excitation time), which is sufficient to separate different isobars from the mixture [2]. As long as the impurity-to-ion ratio is less than one, this procedure is sufficient to remove all impurities. In cases where the ratio is much higher, a dipolar cleaning at the respective modified cyclotron frequency ν_+ of the contaminant becomes essential after the mass-selective buffer gas cooling has been applied. However, also this technique is only applicable for the ratios below a few hundred to one. Furthermore, due to space charge effects the total number of ions manipulated in the ISOLTRAP precision trap should not exceed a thousand.

3.2 Precision Penning trap

From the preparation trap the ion bunch is transferred to the second one, the precision Penning trap, where it

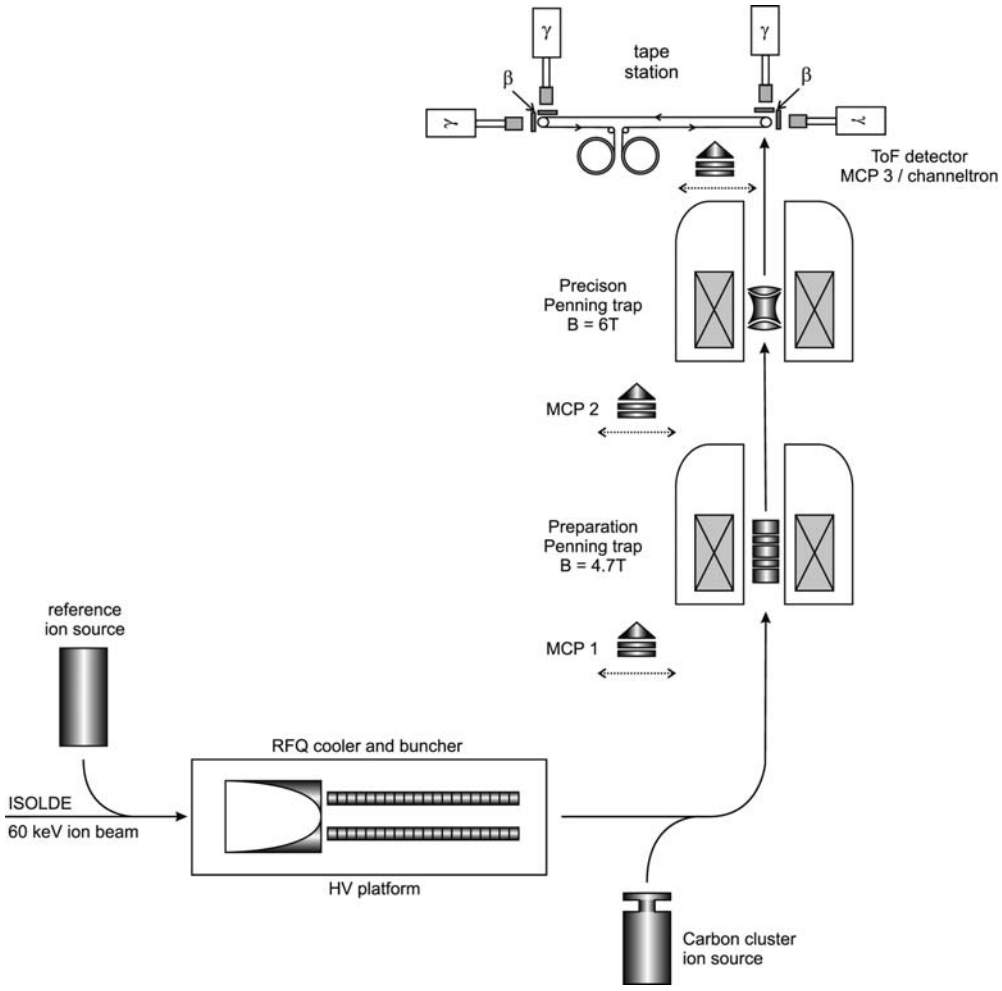

Fig. 2. The triple-trap mass spectrometer ISOLTRAP together with the new tape-transport system for decay studies.

is captured. Here, the mass of the ion is determined, based on its cyclotron frequency ν_c. A resonance spectrum is obtained using the time-of-flight (ToF) ion-cyclotron-resonance technique [30]. The ions are excited with a quadrupole field around ν_c. When the applied frequency corresponds to ν_c, the extra radial energy resulting from the resonant excitation is detected by a reduction in the time of flight of the ions ejected towards a detector (see fig. 4). In order to calibrate the unknown magnetic field at the time of the measurement, the cyclotron frequency of a reference ion with a very well-known mass (^{133}Cs for this study) is measured immediately before and after that of the ion of interest. In this way one can interpolate $\nu_{c,ref}$ in order to obtain the frequency ratio $r = \nu_c/\nu_{c,ref}$. For the standard 1 s excitation the resolving power in this trap is around 4×10^5 while the relative precision in mass determination reaches 1×10^{-8}.

If the resolving power in the preparation trap is not sufficient to prepare a clean beam, additional purification can be performed in the precision trap. Due to its higher resolving power, not only isobaric but even isomeric cleaning [4] is possible here. The removal of contaminants is based on a resonant dipolar excitation at the respective modified cyclotron frequency ν_+ of the contaminants [4]: the radius of the motion increases and the ions hit the trap electrodes. In this way, the amount of contaminant ions can be decreased by at least an additional factor of 10 to 100.

3.3 Decay spectroscopy setup after the precision trap

For the planned decay studies, the ion bunch is first cooled and bunched in the RFQ ion trap and then stored and purified in the preparation Penning trap. If additional purification is required, *e.g.* removal of isomeric contamination, the precision trap is used. Finally, the ions are implanted in a movable tape-transport system, mounted on top of the precision trap (fig. 2). Just in front of the tape the ions are accelerated from 1 keV to around 10 keV using a pulsed electrode to ensure that the implantation is deep enough to prevent the ions from an immediate diffusion. Two modes are envisaged: for ions with half-lives shorter than the minimum proton repetition rate (*i.e.* $t_{1/2}$ below 1.2 s) one ion bunch is implanted at a time and the beta and gamma detection takes place at the implantation point. After a delay corresponding to three half-lives,

the tape is moved by about 1 m to take away the unwanted daughter radioactivity and a new ion bunch is implanted in a clean part of the tape. For ions with a half-life longer than the proton repetition rate it is more efficient to implant several bunches in the same part of the tape. To avoid the loss of ion bunches that are created during the observation of the decay, the tape is moved only after the implantation of the last bunch and the detection takes place around 0.7 m away from the implantation point. During the measurement a new series of ion bunches can be implanted in parallel.

4 Results

4.1 ISOLDE yields with different ion sources

The best material to produce neutron-rich nuclides around ^{208}Pb using proton-induced fragmentation is uranium and thorium. To be extracted and mass-separated the produced atoms need to be ionised. Different ionisation methods are used depending on the element: i) surface ion sources for elements with low ionization potential, ii) plasma/discharge for elements that cannot be surface ionized, and iii) resonant laser excitation [31] (RILIS) allowing particularly high selectivity, applicable in principle to any element.

In the lead region, all elements can be ionised in a plasma. For the ionisation on a hot surface, it is feasible for Fr (ionisation potential of 4.0 eV), followed by Ac (5.2 eV), Ra (5.3 eV), Tl (6.1 eV), Bi (7.3 eV), and Pb (7.4 eV). For the remaining neighbours (Au, Hg, Po, or Rn) surface ionisation at ISOLDE is not possible, because their ionisation potentials are above those of Ta and W (7.6 and 7.9 eV) from which the transfer cavities are commonly made. It is clear that the most efficient surface ionisation takes place for Fr and Ra, and these beams are thus the most disturbing contaminants. Concerning Tl and Hg, surface ionisation is possible only for Tl, whereas the laser ionisation has been used at ISOLDE for both Tl and Hg with efficiencies around 25% and 1%, respectively.

Although much progress has been made on the target and ion source side, none of the presently used methods can fully block Fr and Ra. At the same time other purification methods, such as the use of a neutron converter [32] or extraction as a molecular beam [33], are not suitable for the beams around ^{208}Pb. Ongoing developments to suppress surface-ionised beams make use of laser ionisation. To these belong the use of an ioniser cavity made of a low work-function material [34] or the laser ion source trap (LIST) where the surface-ionised ions are repelled by a positive potential [35]. However, these tools are not yet in standard online operation. Thus, ISOLTRAP is essential for the purification of Tl and Hg beams.

During three ISOLTRAP beamtimes devoted to mass measurements using a UC_x target and different ion sources, we could verify experimentally the production of the neutron-rich Hg and Tl beams, as well as their isobars.

The first beamtime was devoted to masses of neutron-rich Pb isotopes using laser ionisation. Due to technical problems, the yield for Pb isotopes was too low and it was decided to verify the surface ionisation and purification of Tl, Fr and Ra beams. The scan of the mass-selective quadrupole frequency in the preparation trap showed that at $A = 211$ the beam consists —as expected— mostly of Fr and Ra, with traces of Tl, and possibly Pb and Bi. However, the Fr and Ra contamination was so strong that neither Tl nor the other two components could be resolved or purified. (From the number of detected ions with ISOLTRAP, the estimated ISOLDE yields were 10^7–10^9 ions/proton pulse. For technical reasons, the ISOLDE beam gate duration cannot be less than 1 ms so the yield could not be reduced.) The rest of the beamtime was devoted to mass measurements on several Fr and Ra isotopes, which are presented in sect. 4.3.

The second production test used also surface ionisation. It took place during a laser ionisation beamtime on Cd isotopes. This time the UC_x target was coupled to a quartz transfer line which slows down the release of alkali beams, thus reducing their yield [36]. Again, the transfer line does not block the alkali beam totally, necessitating further purification with ISOLTRAP. These tests were also important because the transfer of surface-ionised Tl through the quartz line had never been tested before. Frequency scans of the mass-selective ν_c in the preparation trap for $A = 207$ show that the temperature regime of the transfer line can be chosen such that Fr and Ra retention is assured while Tl is not suppressed. In addition, ^{207}Tl was identified from the mass measurement in the precision trap.

The third test made use of a UC_x target with plasma ionisation coupled to a quartz transfer line for alkali suppression (which had never been tested for Hg transfer). In this case, Fr and Ra were again blocked, but many other isobars were ionised, such as At and Rn. Neutron-rich Tl and Hg isotopes were not visible, even at $A = 209$, in the preparation trap because of the very strong peaks of At and Rn. At the same time, we observed less neutron-rich Tl and Hg ($A = 190, 192, 198$). However, the yield of Hg was smaller closer to stability, which may indicate that the observed Hg ions are not transferred through the quartz line but are created behind the quartz by Tl decay. The application of a quartz transfer line to Hg beams thus requires further investigation.

Based on the above tests, laser ionisation is prefered for Hg, while surface ionisation is also possible for Tl. In addition, the use of the quartz transfer line seems necessary to lower the production of Fr and Ra to a level acceptable for cleaning in the preparation trap. The open questions are: i) can Hg be transferred efficiently through quartz, ii) what are the production rates of Hg and Tl isotopes beyond $N = 126$, and iii) can a ThC_x target give higher yields than UC_x?

4.2 Isobaric cleaning

The capability of purifying isobars in the preparation trap is crucial for the success of ISOLTRAP studies in

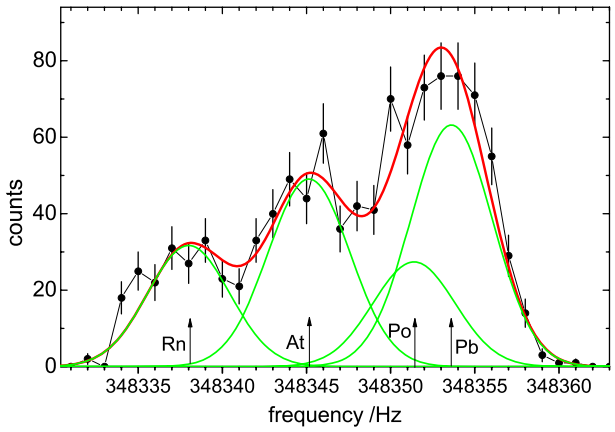

Fig. 3. A mass-selective cooling resonance for the $A = 209$ beam delivered to ISOLTRAP. The fit function consists of four Gaussians of the same width (a free parameter) and fixed peak positions based on the centre of a reference $^{133}Cs^{+}$-resonance.

Table 3. Mass-resolving power $m/\Delta m$ required to separate Hg and Tl isotopes above $A = 208$ from Fr contamination in the ISOLTRAP preparation trap. There are no mass extrapolations available for ions with $A > 212$.

A	$m/\Delta m$ for Hg	$m/\Delta m$ for Tl
208	1.9×10^{4a}	1.4×10^{4}
209	4.3×10^{4a}	2.0×10^{4}
210	1.1×10^{5a}	3.3×10^{4}
211		1.0×10^{5a}
212		1.0×10^{5a}

[a] Based on an extrapolated mass.

the ^{208}Pb region. We have verified this with a UC_x target coupled to the quartz transfer line and plasma ion source, which delivers many different species. The ions were sent through the ISOLDE high-resolution mass separator HRS (with a resolving power $m/\Delta m$ up to 5000) to the ISOLTRAP setup. The frequency scan of the mass-selective quadrupole excitation in the purification trap revealed that the $A = 209$ beam consisted of several species (Rn, At, Pb and/or Po), as shown in fig. 3. Since the width of the resonances is approximately inversely proportional to the duration of the excitation (cooling time), we chose the duration of 1 s which provided a mass-resolving power of over 70 000, enough to resolve Fr from Hg and Tl (see table 3).

To show the cleaning capabilities of ISOLTRAP, the excitation (cooling) time in the preparation trap was reduced to 100 ms so that all isobars were transferred to the precision trap, where the ToF resonance was recorded (fig. 4a) (note that the ions need to be captured and cooled in the preparation trap for efficient injection into the precision trap). Then, the cooling time was increased to 1 s, thus obtaining a 10 times higher mass-resolving power ($m/\Delta m = 70\,000$ should be enough to distinguish between Rn, At, and Pb). Figures 4 b)–d) show results of ToF resonances in the precision trap (with 200 ms excitation time) obtained with the excitation frequency in

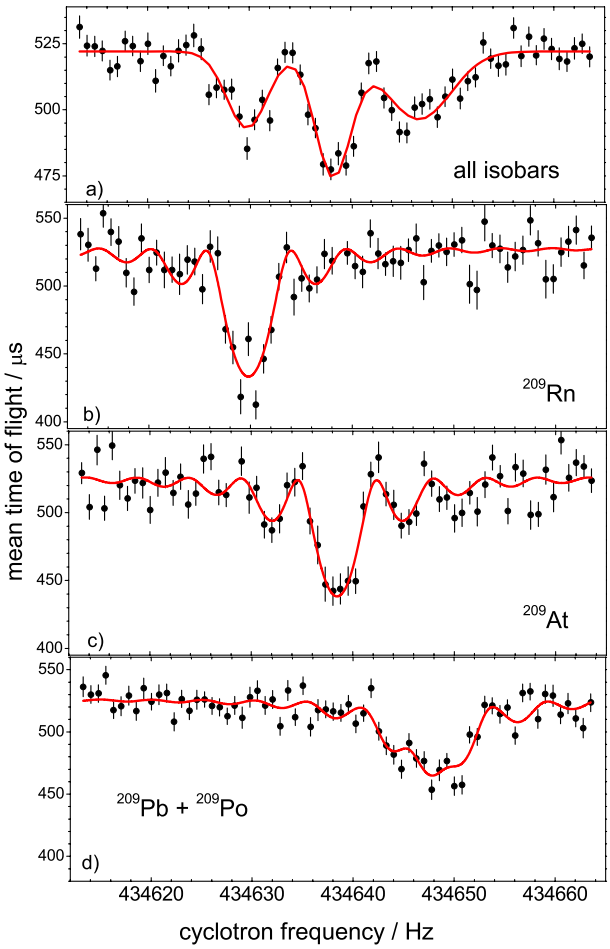

Fig. 4. Time-of-flight resonance curves for several $A = 209$ nuclides: a) with no isobaric cleaning and b)–d) with cleaning. Note the same vertical scale for resonances b)–d) illustrating well that the presence of several species (parts a)) and d)) in the precision trap lowers the signal-to-noise ratio. If ^{209}Tl was present in the beam, its resonance should be visible between those of At and Po.

the preparation trap centered around ^{209}Rn, ^{209}At, and ^{209}Pb, respectively. For Rn and At the spectra show the presence of only one ion species, whereas for Pb the beam clearly consists of two species, which can be identified as ^{209}Pb and ^{209}Po. With longer excitation time in the precision trap, such as the routinely used 1.2 or 2 s, the Po and Pb ToF resonances could be clearly resolved. Also, with additional dipolar cleaning in the precision trap, it should be possible to leave only one species —Po or Pb— in the trap.

4.3 Masses of $^{211-213}$Fr and ^{211}Ra

During one of the production tests using the UC_x target with surface ionisation (described in sect. 4.1) we measured and improved the mass values of several nuclides in the $A = 209$ region. These included $^{211-213}$Fr and ^{211}Ra, with half-lives from 13 s to 20 min and ISOLDE production rates around 10^8 ions per proton pulse for Fr and 10^6

Table 4. Cyclotron-frequency ratios r, using as reference $^{133}Cs^+$ with its mass from AME2003 [12], and mass excess (ME) of $^{211-213}$Fr and ^{211}Ra from AME2003 and from a new AME based on this work (in keV).

Nucl.	Freq. ratio r	ME AME2003	New ME
^{211}Fr	1.587563810 (107)	−4158.3 (21.2)	−4140.1 (11.7)
^{211}Ra	1.587603913 (64)	836.5 (26.2)	832.0 (7.9)
^{212}Fr	1.595092993 (76)	−3537.6 (25.8)	−3516.0 (8.8)
^{213}Fr	1.602616827 (56)	−3549.9 (7.7)	−3553.0 (5.1)

for Ra, making them a problematic contamination. It is important to know these masses as accurately as possible to more quickly and efficiently separate them from those species with yet undetermined masses.

As described in sect. 4.1 Fr and Ra were one of the main constituents of the investigated beams. They could be easily purified using the mass-selective buffer gas centering described in sect. 3, which was visible in large signal-to-noise ratios in the precision trap. In addition, ToF resonances were carefully checked for the presence of any contaminations that might shift the center frequency using a count-rate-class analysis [37]. All resonances were taken with an excitation time of 900 ms or 1.2 s. The theoretical line shape was fitted to the resonance data points [30] in order to extract the cyclotron frequency. The data analysis followed the procedure described in [37]. In addition to the systematic uncertainty of 8×10^{-9}, a relative mass-dependent uncertainty of $1.6{\times}10^{-10}/u(m{-}m_{ref})$ was added to the fit result. $^{133}Cs^+$ ions from the ISOLTRAP offline ion source were used as a reference to derive the cyclotron frequency ratios r, which are presented in table 4. Using r together with the ^{133}Cs mass value [38], a new mass evaluation was performed resulting in the new, more precise, mass excess values presented in table 4. As an additional cross-check, several resonances for ^{208}Pb and ^{238}U were recorded. Both resulting mass excess values agree with literature values to better than 1 keV, however with somewhat larger uncertainties of around 7 keV compared to 1 keV in the Atomic Mass Evaluation 2003 (AME2003).

For ^{211}Fr the AME2003 mass excess value of −4158.3 (21.2) keV was based 81.4% on the mass difference ^{211}Fr-^{226}Ra [39], 17.2% on the α-decay of ^{211}Fr into ^{207}At [40], and 1.4% on the mass difference ^{211}Fr-^{220}Fr and ^{208}Fr [41]. The ISOLTRAP measurement agrees within 1σ with the AME2003 value and contributes 70% to the value of the new AME, −4140.1 (11.7) keV.

In the case of ^{211}Ra, the AME2003 mass excess of 836.5 (26.2) keV was determined only indirectly from two measurements of ^{211}Ra α-decay to ^{207}Rn [42,43], both in agreement. Our value contributes 100% to the new mass excess of 832.0 (7.9) keV and decreases the uncertainty more than three-fold.

The previous ^{212}Fr mass excess −3537.6 (25.8) keV, was 97.2% based on ^{212}Fr-^{226}Ra [39] and 2.8% on ^{212}Fr-^{220}Fr and ^{208}Fr [41]. ISOLTRAP contributes 88.5% to the new mass excess of −3516.0 (8.8) keV and shifts it by 22 keV.

Table 5. Mass excess values (keV) influenced by measurements on $^{211-213}$Fr and ^{211}Ra presented in this article, before [12] and after our studies.

Nuclide	ME AME2003	New ME	ME shift
^{199}Pb	−25228.0 (26.4)	−25232.5 (10.2)	−4.5
^{203}Bi	−21540.4 (21.8)	−21522.6 (12.9)	17.9
^{203}Po	−17307.1 (25.9)	−17311.6 (8.8)	−4.5
^{204}Bi	−20667.3 (26.0)	−20645.7 (9.2)	21.6
^{205}Bi	−21061.8 (7.2)	−21064.4 (5.2)	−2.6
^{207}At	−13243.2 (21.6)	−13225.2 (12.6)	18.0
^{207}Rn	−8631.0 (26.0)	−8635.5 (8.7)	−4.5
^{208}At	−12491.4 (25.9)	−12469.8 (8.9)	21.6
^{209}At	−12879.7 (7.5)	−12882.6 (5.2)	−2.9
^{215}Ac	6010.9 (21.6)	6029.1 (12.2)	18.1
^{215}Th	10926.7 (26.9)	10922.2 (9.8)	−4.5
^{216}Ac	8122.7 (26.6)	8144.3 (10.8)	21.6
^{216}Ac^m	8166.3 (26.1)	8187.9 (9.5)	21.6
^{217}Ac	8706.5 (12.8)	8703.5 (11.4)	−3.0
^{217}Ac^m	10718.7 (18.9)	10715.7 (18.1)	−3.0
^{219}Pa	18520.5 (54.4)	18538.6 (51.5)	18.1
^{219}U	23212.0 (56.8)	23207.6 (51.0)	−4.5
^{220}Pa	20376.7 (56.6)	20398.3 (51.2)	21.6
^{221}Pa	20379.1 (51.6)	20376.1 (51.3)	−3.0
^{225}Np	31590.5 (71.9)	31587.5 (71.6)	−3.0

Two measurements of the α-decay of ^{213}Fr to ^{209}At [40,44] completely determined the mass excess of ^{213}Fr, yielding −3549.9 (7.7) keV. Our result contributes 55.3% to the new mass excess of −3553.0 (5.1) keV, and decreases the uncertainty by almost a factor of two.

The new masses of $^{211-213}$Fr and ^{211}Ra influence over 20 other masses, shown in fig. 5, that are connected via α-decay chains or nuclear reactions. In some cases the mass uncertainty decreased even three-fold. Previous and new masses, derived from a new Atomic Mass Evaluation are presented in table 5. This list does not include mass excess values influenced by the new ^{208}Fr mass (due to $^{212-213}$Fr changes: ^{208}Fr, ^{212}Ac, ^{216}Pa) which increased by only 1.6 keV with no change in uncertainty. Also the influence on $^{219-220}$Pa and ^{219}U masses is almost negligible.

5 Summary

The inherently high resolving power of Penning traps [45] allows using them for precision studies on isobarically and even isomerically pure beams. Using the Penning trap mass spectrometer ISOLTRAP we have performed preparatory studies for mass and decay studies of neutron-rich Hg and Tl isotopes beyond $N = 126$, which are poorly known since they are delivered with large isobaric contam-

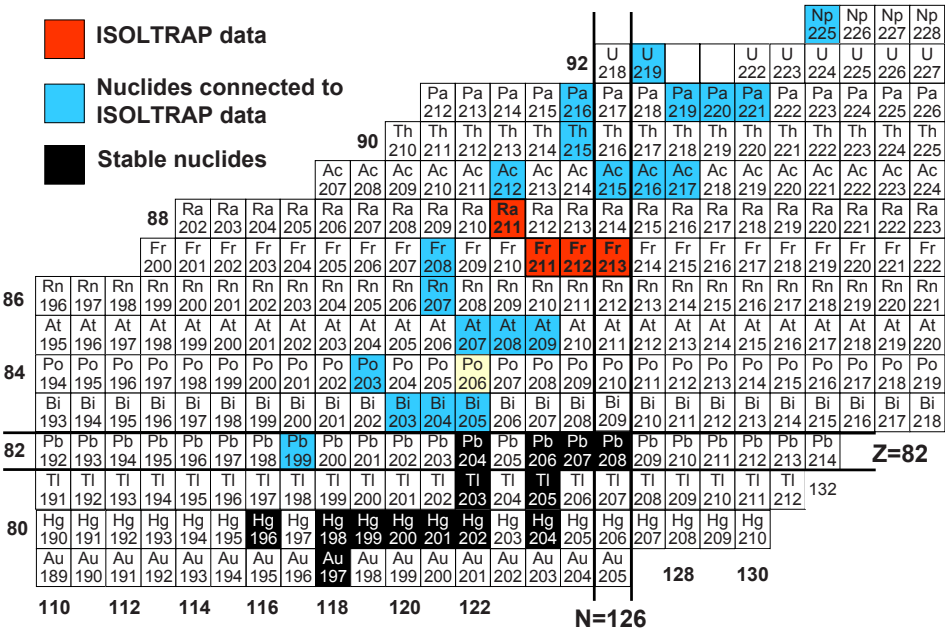

Fig. 5. (Colour on-line) Nuclear chart around ^{208}Pb including nuclides investigated by ISOLTRAP whose new masses are presented in this article (in red and bold) and nuclides with masses influenced by our new data (in blue).

ination of surface-ionised Fr. The recent production tests show that specific ionisation schemes (laser for Tl and Hg or surface for Tl), together with the use of the quartz line to filter the alkali isobars, can provide a beam that can be purified further with ISOLTRAP. Furthermore, the resolving power of over 70 000 that is required to purify Fr has been achieved for masses around $A = 208$ in the ISOLTRAP purification trap. Masses of several nuclides in this region, $^{211-213}$Fr and ^{211}Ra, have been determined with about 3 times better precision than previously. Exact values of contaminant masses are important in order to quickly and efficiently separate them from the more weakly produced exotic species having unknown masses. The new masses influence over 20 other masses in the ^{208}Pb region, and bring down many mass excess uncertainties below 10 keV. Further tests of the production of Tl and Hg beams beyond $N = 126$ are required before the measurements of interest can be performed. Next steps include also the comissioning of a tape-transport system with radioactive beam.

This work was supported by the German Federal Ministry for Education and Research (BMBF) (06GF186I, 06MZ215), Helmholtz Association for National Research Centers (VH-NG-037), the French IN2P3, the Spanish MICINN (FPA-2007-62216), and the EU FP6 programme (MEIF-CT-2006-042114 and RII3-EURONS 506065). We are grateful to the ISOLDE technical group for their support.

References

1. L. Schweikhard, G. Bollen (Editors), Int. J. Mass Spectrom. **251**, issue 2/3 (2006).
2. H. Raimbault-Hartmann *et al.*, Nucl. Instrum. Methods B **126**, 378 (1997).
3. D. Beck *et al.*, Nucl. Instrum. Methods B **126**, 374 (1997).
4. K. Blaum *et al.*, Europhys. Lett. **67**, 586 (2004).
5. J.V. Roosbroeck *et al.*, Phys. Rev. Lett. **92**, 112501 (2004).
6. S. Rinta-Antila *et al.*, Eur. Phys. J. A **31**, 1 (2007).
7. M. Block *et al.*, Phys. Rev. Lett. **100**, 132501 (2008).
8. D. Neidherr *et al.*, Phys. Rev. Lett. **102**, 112501 (2009).
9. P. Möller *et al.*, At. Data Nucl. Data Tables **66**, 131 (1997).
10. I. Borzov, Phys. Rev. C **67**, 025802 (2003).
11. C. Weber *et al.*, Nucl. Phys. A **803**, 1 (2008).
12. G. Audi, A. Wapstra, C. Thibault, Nucl. Phys. A **729**, 337 (2003).
13. L. Chen *et al.*, Phys. Rev. Lett. **102**, 122503 (2009).
14. J. Jänecke, T. O'Donnell, Nucl. Phys. A **781**, 317 (2007).
15. J.-Y. Zhang *et al.*, in *Proceedings of the International Conference on Contemporary Topics in Nuclear Structure in Cocoyoc, Mexico*, Vol. **109**, C65 (1988) (unpublished).
16. J.-Y. Zhang, R.F. Casten, D.S. Brenner, Phys. Lett. B **227**, 1 (1989).
17. M. Stoitsov *et al.*, Phys. Rev. Lett. **98**, 132502 (2007).
18. I. Talmi, Rev. Mod. Phys. **34**, 704 (1962).
19. S. Schwarz *et al.*, Nucl. Phys. A **693**, 533 (2001).
20. L. Zhang *et al.*, Eur. Phys. J. A **16**, 299 (2003).
21. M. Pfützner *et al.*, Phys. Lett. B **444**, 32 (1998).
22. R. Firestone *et al.*, *Table of Isotopes*, 1999 update (Wiley, 1999).
23. L. Zhang *et al.*, Phys. Rev. C **58**, 156 (2004).
24. T. Kuo, G. Herling, US Naval Research Laboratory, Report No. 2258 (1971).
25. K. Maier, Acta Phys. Pol. B **32**, 899 (2001).
26. K. Maier, M. Rejmund, Eur. Phys. J. A **14**, 349 (2002).
27. M. Mukherjee *et al.*, Eur. Phys. J. A **35**, 1 (2008).
28. F. Herfurth *et al.*, Nucl. Instrum. Methods A **469**, 254 (2001).
29. G. Savard *et al.*, Phys. Lett. B **158**, 247 (1991).

30. M. König *et al.*, Int. J. Mass Spectrom. Ion Process. **142**, 95 (1995).
31. V. Fedosseev *et al.*, Nucl. Instrum. Methods B **204**, 353 (2003).
32. U. Köster, Eur. Phys. J. A **15**, 255 (2002).
33. D. Stracener, Nucl. Instrum. Methods B **204**, 42 (2003).
34. M. Mena *et al.*, Nucl. Instrum. Methods B **266**, 4391 (2008).
35. F. Schwellnus *et al.*, Nucl. Instrum. Methods B **266**, 4383 (2008).
36. E. Bouquerel *et al.*, Nucl. Instrum. Methods B **266**, 4298 (2008).
37. A. Kellerbauer *et al.*, Eur. Phys. J. A **22**, 53 (2003).
38. M. Bradley *et al.*, Phys. Rev. Lett. **83**, 4510 (1999).
39. G. Bollen *et al.*, J. Mod. Opt. **39**, 257 (1992).
40. K. Valli, E.K. Hyde, W. Treytl, J. Inorg. Nucl. Chem. **29**, 2503 (1967).
41. G. Audi *et al.*, Nucl. Phys. A **378**, 443 (1982).
42. K. Valli, W. Treytl, E.K. Hyde, Phys. Rev. **161**, 1284 (1967).
43. F.P. Heßberger, S. Hofmann, D. Ackermann, Eur. Phys. J. A **16**, 365 (2003).
44. P. Hornshøj, P.G. Hansen, B. Jonson, Nucl. Phys. A **230**, 380 (1974).
45. K. Blaum, Phys. Rep. **425**, 1 (2006).